



# Transcriptional Regulation of *icaADBC* by both IcaR and TcaR in *Staphylococcus epidermidis*

Tra-My Hoang,<sup>a</sup> C. Zhou,<sup>a</sup> J. K. Lindgren,<sup>a</sup> M. R. Galac,<sup>b</sup> B. Corey,<sup>b</sup> J. E. Endres,<sup>a</sup> M. E. Olson,<sup>c</sup> P. D. Fey<sup>a</sup>

<sup>a</sup>Department of Pathology and Microbiology, University of Nebraska Medical Center, Omaha, Nebraska, USA

<sup>b</sup>Multidrug-Resistant Organism Repository and Surveillance Network (MRSN), Walter Reed Army Institute of Research, Silver Spring, Maryland, USA

<sup>c</sup>Department of Medical Microbiology, Immunology and Cell Biology, Southern Illinois University School of Medicine, Springfield, Illinois, USA

**ABSTRACT** *S. epidermidis* is a primary cause of biofilm-mediated infections in humans due to adherence to foreign bodies. A major staphylococcal biofilm accumulation molecule is polysaccharide intracellular adhesin (PIA), which is synthesized by enzymes encoded by the *icaADBC* operon. Expression of PIA is highly variable among clinical isolates, suggesting that PIA expression levels are selected in certain niches of the host. However, the mechanisms that govern enhanced *icaADBC* transcription and PIA synthesis in these isolates are not known. We hypothesized that enhanced PIA synthesis in these isolates was due to function of IcaR and/or TcaR. Thus, two *S. epidermidis* isolates (1457 and CSF41498) with different *icaADBC* transcription and PIA expression levels were studied. Constitutive expression of both *icaR* and *tcaR* demonstrated that both repressors are functional and can completely repress *icaADBC* transcription in both 1457 and CSF41498. However, it was found that IcaR was the primary repressor for CSF41498 and TcaR was the primary repressor for 1457. Further analysis demonstrated that *icaR* transcription was repressed in 1457 in comparison to CSF41498, suggesting that TcaR functions as a repressor only in the absence of IcaR. Indeed, DNase I footprinting suggests IcaR and TcaR may bind to the same site within the *icaR-icaA* intergenic region. Lastly, we found mutants expressing variable amounts of PIA could rapidly be selected from both 1457 and CSF41498. Collectively, we propose that strains producing enhanced PIA synthesis are selected within certain niches of the host through several genetic mechanisms that function to repress *icaR* transcription, thus increasing PIA synthesis.

**IMPORTANCE** *Staphylococcus epidermidis* is a commensal bacterium that resides on our skin. As a commensal, it protects humans from bacterial pathogens through a variety of mechanisms. However, it is also a significant cause of biofilm infections due to its ability to bind to plastic. Polysaccharide intercellular adhesin is a significant component of biofilm, and we propose that the expression of this polysaccharide is beneficial in certain host niches, such as providing extra strength when the bacterium is colonizing the lumen of a catheter, and detrimental in others, such as colonization of the skin surface. We show here that fine-tuning of *icaADBC* transcription, and thus PIA synthesis, is mediated via two transcriptional repressors, IcaR and TcaR.

**KEYWORDS** *Staphylococcus epidermidis*, biofilms, transcriptional regulation

*Staphylococcus epidermidis* colonizes the human skin, especially the axillae, head, legs, arms, and nares (1). In this environment, *S. epidermidis* is considered a commensal organism and is thought to be beneficial to the human host by preventing colonization of pathogens via intra- and interspecies competition (2, 3). *S. epidermidis* has also been shown to influence the host immune response, resulting in enhanced innate immunity against more pathogenic species (4). However, due to its ability to bind foreign

**Citation** Hoang T-M, Zhou C, Lindgren JK, Galac MR, Corey B, Endres JE, Olson ME, Fey PD. 2019. Transcriptional regulation of *icaADBC* by both IcaR and TcaR in *Staphylococcus epidermidis*. *J Bacteriol* 201:e00524-18. <https://doi.org/10.1128/JB.00524-18>.

**Editor** George O'Toole, Geisel School of Medicine at Dartmouth

**Copyright** © 2019 American Society for Microbiology. All Rights Reserved.

Address correspondence to P. D. Fey, pfey@unmc.edu.

**Received** 28 August 2018

**Accepted** 17 December 2018

**Accepted manuscript posted online** 2 January 2019

**Published** 25 February 2019

bodies, *S. epidermidis* is the fourth leading cause of hospital-acquired infections, accounting for 22% of bloodstream infections in ICU patients, and mediates 30 to 43% of prosthetic joint infections (5–9).

*S. epidermidis* infections are characterized by the formation of biofilms (10). Biofilms form on damaged host tissues or surgically implanted medical devices and are generally defined as complex, three-dimensional communities of cells, surrounded by a matrix (11, 12). Due to their structure and the quiescent state of cells within a biofilm, biofilm infections are known to be resistant to antimicrobials, as well as the host immune system (13–15). Biofilms form on the surface of medical implant devices such as catheters, knee and hip joints, as well as cerebrospinal fluid (CSF) shunts. The formation of biofilms is commonly described as a multistep process consisting of adherence, multiplication, exodus, maturation, and dispersal (16, 17). This process involves many factors, including proteins, extracellular DNA, teichoic acids, polysaccharides, nucleases, and proteases (12, 18–24). Polysaccharide intercellular adhesin (PIA) has been well described in the literature as an accumulation molecule utilized during *S. epidermidis* biofilm formation (11, 21, 22, 25–43). Although *S. epidermidis* produces other molecules (Aap, Embp, Bap, etc.) that function in biofilm accumulation (44–48), PIA synthesis enhances virulence as evident using models of implant-related infection (37–39). Further, other investigators have found that shear flow induces PIA synthesis in both *S. epidermidis* and *S. aureus*, suggesting that PIA may function to protect the biofilm structure during shear stress (5, 48, 49). Indeed, our laboratory recently reported that *S. epidermidis* isolates collected from catheter-related infections more often produced significant levels of PIA, suggesting that mutants with enhanced PIA synthesis may be selected during high shear stress, such as the lumen of a catheter. Furthermore, it has been well documented that there is wide variation in the amounts of PIA produced by different *S. epidermidis* clinical strains, and those strains producing significant amounts of PIA are phenotypically noted as producing enhanced biofilm in *in vitro* biofilm tests (43, 50–55). However, it is unclear how this wide variation in PIA synthesis is regulated.

The *icaADBC* operon, which encodes the enzymes responsible for the synthesis of PIA, was originally identified from experiments using transposon mutagenesis to isolate *S. epidermidis* mutants unable to form biofilm (56–58). PIA is a partially N-acetylated  $\beta$ -1,6-linked poly-N-acetyl-D-glucosamine (PNAG) polymer (28, 31, 56). *icaADBC* transcription has been shown to be regulated by a multitude of growth conditions, as well as by various transcriptional regulators, including IcaR, TcaR, SarA, and the  $\sigma$  factor  $\sigma^B$  (11, 59–66).

Upstream of and divergently transcribed from the *icaADBC* promoter is *icaR*, a member of the TetR family of transcriptional regulators encoding a transcriptional repressor of the *ica* operon (59). IcaR functions by binding to a specific DNA sequence immediately upstream of *icaA* (67). Regulation of *icaR* itself is not well understood, although the alternative sigma factor  $\sigma^B$  has been shown to indirectly repress *icaR* transcription (64). Transcription of *icaR* has been shown to also be repressed by 10% NaCl and 4% ethanol (68), perhaps due to the involvement of  $\sigma^B$  and its function as a stress response  $\sigma$  factor.

In addition to IcaR, a second direct repressor of *icaADBC* was identified in *S. aureus*. The regulator, named TcaR (teicoplanin-associated locus regulator), belongs to the MarR family of transcriptional regulators which function in teicoplanin and methicillin resistance (69), as well as regulation of a number of genes including *spa*, *sasF*, *sarS*, and *icaADBC* (63, 70, 71). Putative binding sequences have been identified in the promoter region of the *ica* operon, suggesting that TcaR functions as a direct repressor (72, 73). However, functional studies of TcaR in regulating *icaADBC* expression, PIA synthesis, and biofilm formation have not been reported in *S. epidermidis*.

We report here that both IcaR and TcaR function to repress *icaADBC* transcription in *S. epidermidis* and show that IcaR is transcriptionally repressed in 1457, a strain that produces enhanced PIA. Thus, mutations that function to repress IcaR transcription may be selected in high shear environments to allow for enhanced binding capability.

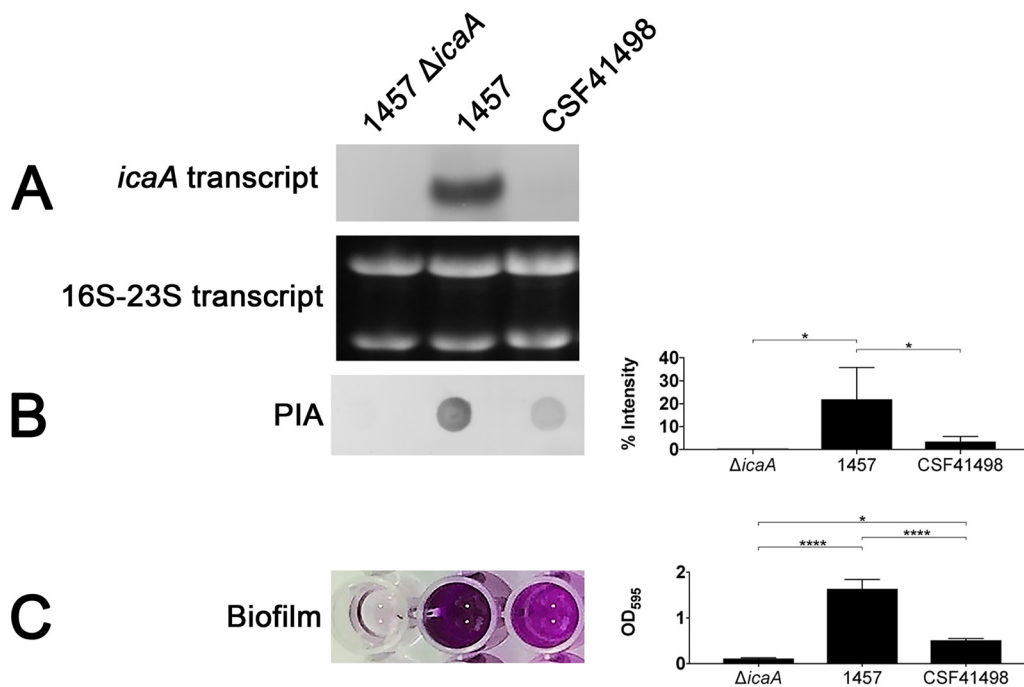


**FIG 1** *S. epidermidis* 1457 and CSF41498 differ in *icaA* transcription, PIA synthesis, and biofilm formation. In comparison to 1457, less *icaA* transcript (A), PIA (B), and biofilm (C) was detected in CSF41498. RNA was isolated from the mid-exponential phase during microaerobic growth (5:3 flask to volume ratio; 125 rpm, 37°C). PIA was purified from the post-exponential phase. Biofilm was stained with crystal violet after 24 h of growth in TSB. RNA gel shown as a loading control. PIA dot blot and biofilm analyses were assessed using three biological replicates.

## RESULTS

***S. epidermidis* strains 1457 and CSF41498 differ in *icaA* transcript, PIA synthesis, and *in vitro* biofilm formation.** Our previous results and those of others (36, 43, 48, 74–76) have documented that biofilm/PIA levels are variable among clinical isolates of *S. epidermidis* and enhanced biofilm formation correlates with increased *icaA* transcript and enhanced PIA synthesis. We chose to study strains 1457 and CSF41498, two genetically amenable clinical strains that differ in their *in vitro* biofilm production and synthesis of PIA. As shown in Fig. 1A, an enhanced *icaA* transcript is detected in strain 1457 compared to the strains 1457  $\Delta$ *icaA* and CSF41498. In addition, strain 1457 produces more PIA, as detected by immunoblotting (Fig. 1B), in addition to *in vitro* biofilm, as assessed using a Christensen biofilm assay (Fig. 1C).

**Both *IcaR* and *TcaR* regulate *icaADBC* transcription.** *IcaR* is a direct repressor of *icaADBC* in both *S. aureus* and *S. epidermidis* (59, 61, 63, 68); however, the function of *TcaR* is less understood. Based on the observation that PIA synthesis and *icaA* transcription were variable in clinical isolates of *S. epidermidis*, we hypothesized that *IcaR* and/or *TcaR* was nonfunctional in strains producing excess PIA such as strain 1457. Bioinformatic analyses of the 1457 and CSF41498 genomes (accession numbers CP020463.1 and CP030246) showed no sequence divergence in *icaR*, *tcaR*, *icaADBC*, or the *icaR-icaA* intergenic region. *icaR* and *tcaR* allelic replacement mutants were constructed in both 1457 and CSF41498 and biofilm production, PIA synthesis and *icaA* transcription were assessed. Consistent with previous results, deletion of *icaR* in CSF41498 resulted in increased *icaA* transcription and enhanced biofilm and PIA synthesis (Fig. 2B, C, and E) (59, 68). However, in contrast to CSF41498, inactivation of *icaR* in *S. epidermidis* 1457 resulted in no significant difference in *icaA* transcription or biofilm production, and PIA synthesis decreased slightly (Fig. 2A, C, and E). We also observed opposite phenotypes when the *tcaR* mutants of 1457 and CSF41498 were compared. In strain 1457, enhanced *icaA* transcript, PIA synthesis, and biofilm production were detected (Fig. 2A, C, and E). In contrast, no significant changes were noted in

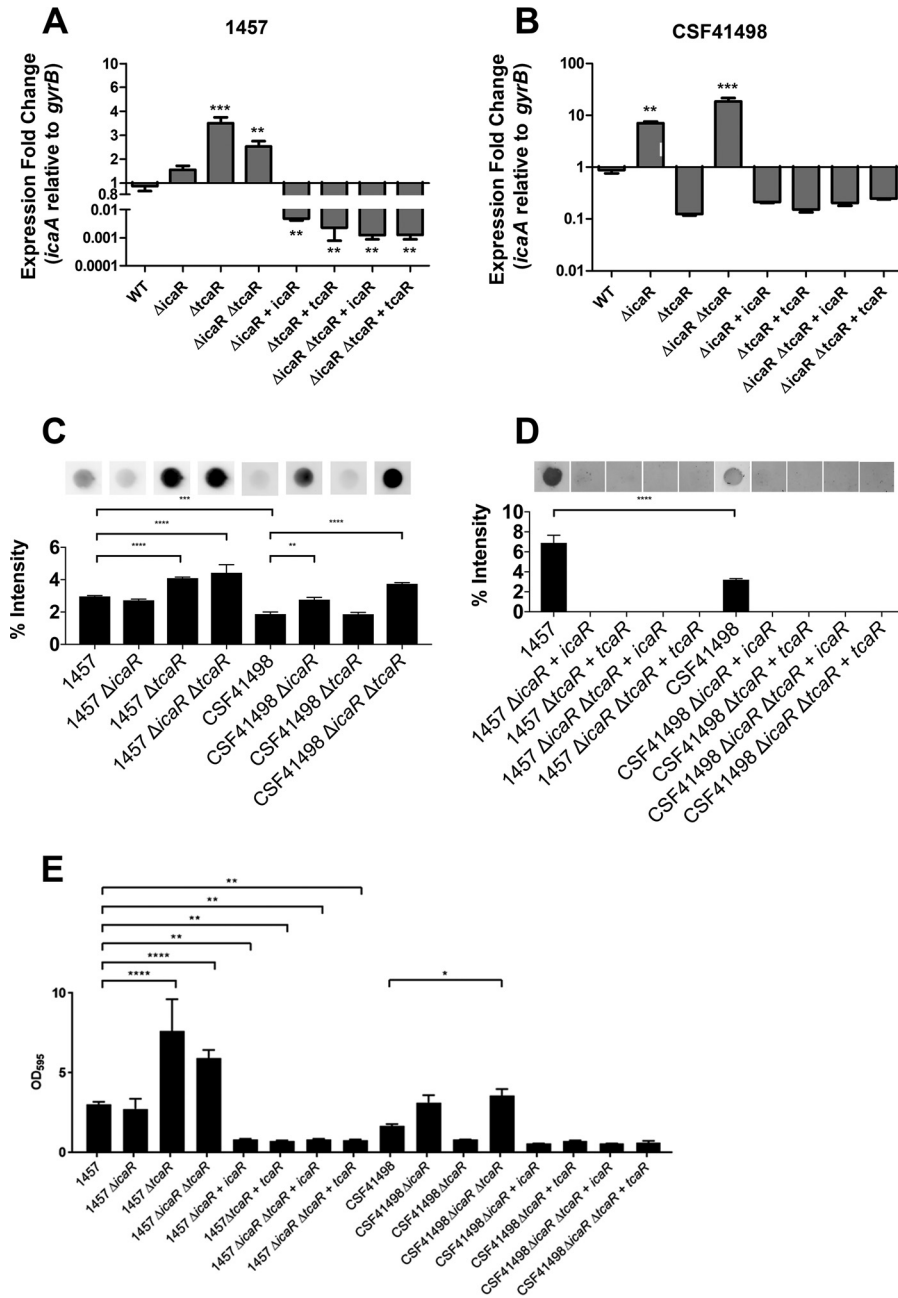


**FIG 2** *icaA* transcription, PIA synthesis, and biofilm production in 1457 and CSF41498. (A and B) Quantitative real-time PCR was performed to evaluate *icaA* transcription in 1457 (A) and CSF41498 (B)  $\Delta$ icaR,  $\Delta$ tcaR,  $\Delta$ icaR  $\Delta$ tcaR, and constitutive *icaR* and *tcaR* cis complement strains. *icaA* (3310 and 3311) and *gyrB* (2301 and 2302) specific primers were used. *icaA* expression was calculated relative to *gyrB*, and all strains were compared to the wild type. RNA was isolated in the mid-exponential phase during microaerobic growth (5:3 flask/volume ratio; 125 rpm, 37°C). One-way analysis of variance (ANOVA) was performed, followed by Dunnett’s multiple-comparison test, to determine significance; all groups were compared to the wild type. \*\*,  $P \leq 0.01$ ; \*\*\*,  $P \leq 0.001$ . (C and D) PIA was purified from the post-exponential phase and detected using a PIA-specific antibody. The percent intensity was measured using ImageJ software. (E) Biofilm formation was determined using a Christensen biofilm assay and assessed based on the OD<sub>595</sub>. Statistical analysis for panels C, D, and E was performed using one-way ANOVA with Tukey’s multiple-comparison test. \*,  $P \leq 0.05$ ; \*\*,  $P \leq 0.01$ ; \*\*\*,  $P \leq 0.001$ ; \*\*\*\*,  $P \leq 0.0001$ . PIA dot blot and biofilm analyses were assessed using three biological replicates.

the CSF41498  $\Delta$ tcaR strain with respect to PIA synthesis or biofilm production and a decrease in *icaA* transcript was detected by quantitative reverse transcription-PCR (qRT-PCR) (Fig. 2B, C, and E). However, similar phenotypes were observed when the  $\Delta$ icaR  $\Delta$ tcaR mutants were compared between 1457 and CSF41498; both strains

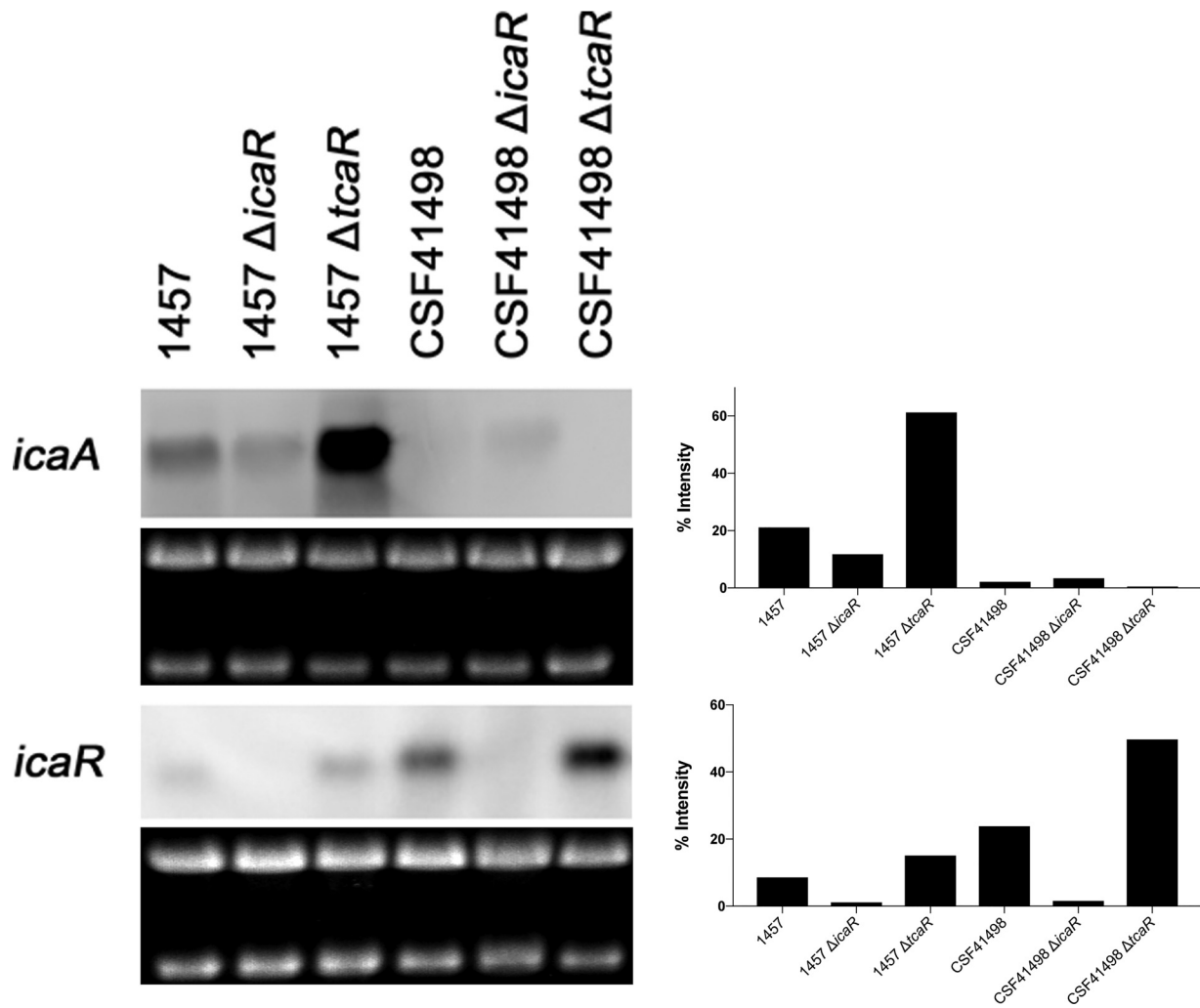


**FIG 3** *icaR* transcription in 1457 and CSF41498. Northern blot analyses of *icaA* and *icaR* transcripts in 1457 and CSF41498 and mutants were performed. Transcript was detected using a DIG-labeled *icaA* or *icaR* DNA probe. Total RNA was isolated in the mid-exponential phase after microaerobic growth (5:3 flask/volume ratio; 125 rpm, 37°C). The percent intensity was measured using ImageJ software. An RNA gel is shown as a loading control.

produced enhanced *icaA* transcript, PIA synthesis, and biofilm production (Fig. 2A, B, C, and E). Collectively, these data suggest that both IcaR and TcaR function to regulate *icaADBC* transcription.

Based on the fact that the 1457  $\Delta$ *icaR* mutant yielded only a slight phenotype, we predicted that *icaR* may not be transcriptionally active in this strain. Indeed, transcriptional analysis of both 1457 and CSF41498 demonstrated that less *icaR* transcript was detected in 1457 in comparison to CSF41498 (Fig. 3). Further, we constructed plasmids encoding 1457 *icaR* (pNF332) or *tcaR* (pNF333) that were controlled by a constitutive *sarA* promoter (77). Both pNF332 and pNF333 were integrated into the *S. epidermidis* chromosomal lipase gene of both  $\Delta$ *icaR* and  $\Delta$ *tcaR* mutants, respectively, using allelic replacement methodologies. These data demonstrated that overexpression of IcaR or TcaR in the 1457 or CSF41498 background resulted in complete repression of *icaA* transcript, PIA synthesis, or biofilm production (Fig. 2A, B, D, and E). In addition, when pNF332 and pNF333 were integrated into 1457  $\Delta$ *icaR*  $\Delta$ *tcaR* and CSF41498  $\Delta$ *icaR*  $\Delta$ *tcaR* strains, constitutive expression of either IcaR or TcaR again resulted in complete repression of *icaA* transcript, PIA synthesis, and biofilm production (Fig. 2A, B, D, and E). Collectively, these data suggest that both IcaR and TcaR function as a repressor of *icaADBC* transcription. When overproduced, both proteins can effectively abolish

*icaADBC* transcription, PIA synthesis, and biofilm formation. However, when IcaR is expressed at sufficient levels, such as in CSF41498, it effectively represses *icaADBC* transcription and TcaR has little functional role in *icaADBC* transcription. However, when IcaR concentration is reduced, such as in strain 1457, TcaR functions as a repressor of *icaADBC*, suggesting that IcaR is the major repressor. In addition, these data may suggest that IcaR and TcaR may have overlapping binding sites in the *icaR-icaA* intergenic region.

Lastly, it was noted that a decrease in *icaA* transcript was detected in the CSF41498  $\Delta tcaR$  strain, suggesting that TcaR may function to repress *icaR* transcription (Fig. 2B and 3). Therefore, Northern analyses were performed to determine *icaR* transcript in the 1457 and CSF41498  $\Delta tcaR$  mutants. We observed a slight increase in the detection of *icaR* transcript in the *tcaR* mutant in both 1457 and CSF41498 (Fig. 3). These data are corroborated by previous work identifying a TcaR binding site located within the *icaR* promoter (72) and show that TcaR not only functions as a repressor of *icaADBC* transcription but also functions as a repressor of *icaR*. It was tempting to speculate that enhanced *tcaR* transcription was noted in 1457, in comparison to CSF41498, allowing for decreased *icaR* transcription. However, RT-PCR analyses noted that there was no significant difference in *tcaR* transcription suggesting that *tcaR* is not transcriptionally upregulated in 1457, facilitating decreased *icaR* transcription (see Fig. S1 in the supplemental material).

**TcaR binds to multiple sequences in the *icaR-icaA* intergenic region.** Since IcaR and TcaR are known to bind to the *icaR-icaA* intergenic region (67, 78), DNase I footprinting assays were performed to determine whether both bind to similar DNA sequences within the *icaR-icaA* intergenic region. As expected, binding of IcaR to the DNA resulted in a protected region just upstream of the *icaA* start site (Fig. 4), confirming previous DNase I footprinting results that IcaR bound to a 42-bp sequence in the *ica* promoter (78). The addition of TcaR resulted in the partial protection of three regions within the *icaR-icaA* intergenic region, one of which overlapped with the *icaR* binding region. Previous data found that TcaR binds to three sites within the *icaR-icaA* intergenic region (63, 72). Although previous electrophoretic mobility shift assays (EMSA) demonstrated that TcaR bound just upstream of the *icaR* start site (TcaR binding site 1) (Fig. 4), we were unable to observe a clear binding area within this region. However, we did observe binding to the 2nd and 3rd TcaR binding regions in addition to a binding region within the IcaR binding site. It is important to note that the proposed *icaR* promoter is found within TcaR binding region 2. Taken together, our data show that TcaR binds to at least three sites within the *icaR-icaA* intergenic region and may bind to the same region as IcaR.

**Selection of mutants that facilitate altered PIA synthesis in 1457 and CSF41498.** Previous studies have hypothesized that mutations which facilitate enhanced PIA synthesis are selected to allow for colonization in high shear stress niches such as the lumen of a catheter (22, 74). Based on our studies with 1457, it is possible that some of these mutations mediate decreased *icaR* transcription, resulting in increased PIA synthesis. To identify potential mutations that mediate increased PIA synthesis, CSF41498 was grown in tissue culture flasks, and the medium, tryptic soy broth (TSB), was replaced daily for 5 days to select for mutations that facilitate adherence to the plastic. On day 5, Congo red agar (CRA) was used to identify CSF41498 mutants with enhanced PIA synthesis (colonies appear crusty instead of smooth) (Fig. 5A) (79). In a similar manner, to identify 1457 mutants that produce decreased PIA, 1457 was grown in biofilm flow cells (Stovall) and plated on CRA after 5 days to isolate smooth colonies as previously described (22). In addition, 1457 smooth mutants were isolated from a guinea pig tissue cage model as previously described (80).

A total of 10 CSF41498 mutants with increased PIA and biofilm formation were isolated, and six were selected for further analysis (A9, P4, C9, D9, N2, and O7). We observed highly variable phenotypes with all six of these mutants with regard to *icaA/icaR* transcriptional analysis and PIA/biofilm synthesis (Fig. 5B and C). Enhanced *icaA* transcription was detected in all six mutants, and other than mutant P4, all of them showed increased biofilm/PIA

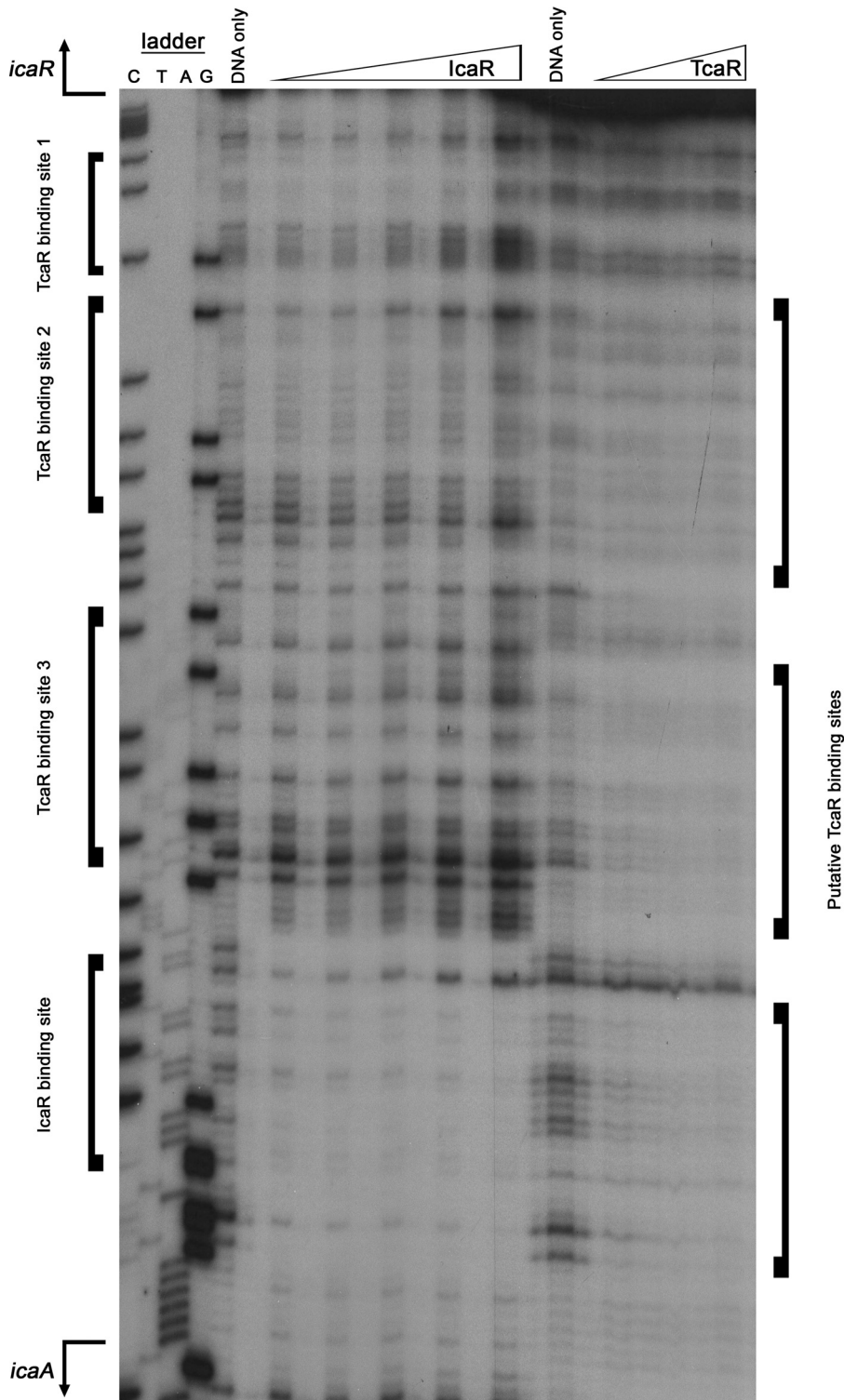


**FIG 4** TcaR binds to multiple sites in the *icaR-icaA* intergenic region. Incubation with IcaR resulted in a footprint upstream of *icaA*. Incubation with TcaR resulted in a footprint throughout the intergenic region (three sites noted on the right). <sup>32</sup>P-labeled *icaR-icaA* intergenic DNA (amplified with the primers 2855 and 2965) was incubated with increasing concentrations of recombinant IcaR or TcaR, treated with DNase I, and electrophoresed on a 6% denaturing polyacrylamide gel. Previously proposed TcaR binding sites and experimentally derived IcaR binding site are noted on the left.

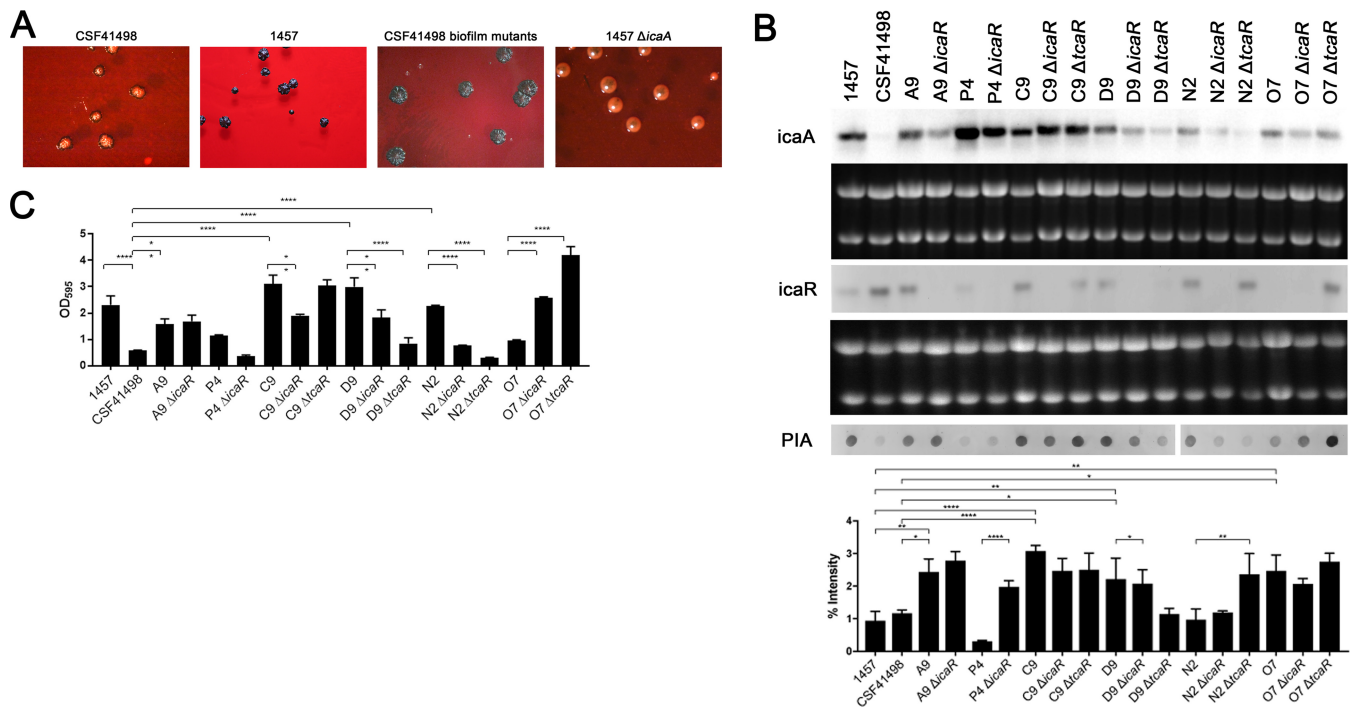


**FIG 5** *icaA* transcription, PIA synthesis and biofilm production in CSF41498 enhanced biofilm mutants. CSF41498 was screened on Congo red agar (CRA) after selection for enhanced adherence. Strains not producing PIA, such as the 1457  $\Delta$ icaA mutant, have a smooth, round phenotype on CRA, whereas strains that produce significant amounts of PIA, such as 1457, appear crusty and rough on CRA. CSF41498 has an intermediate phenotype on CRA. (A) CSF41498 mutants selected on CRA have a colony phenotype similar to 1457. (B and C) Northern blot analyses detecting *icaA* and *icaR* transcript in CSF41498 biofilm mutants in addition to PIA synthesis (B) and biofilm formation (C) compared to CSF41498 wild type (WT). Statistical analysis was performed using one-way ANOVA with Tukey's multiple-comparison test. \*,  $P \leq 0.05$ ; \*\*,  $P \leq 0.01$ ; \*\*\*,  $P \leq 0.001$ ; \*\*\*\*,  $P \leq 0.0001$ . An RNA gel is shown as a loading control. PIA dot blot and biofilm analyses were assessed from three biological replicates.

synthesis. Based on our observations with 1457, we expected that some of the mutants would display decreased *icaR* expression. Indeed, less *icaR* transcript was detected in mutants P4 and O7. Of particular interest was mutant O7 since it displayed the most similar phenotype with that observed in strain 1457. No *icaR* was detected in mutant O7, and a more pronounced biofilm/PIA phenotype was observed in the *tcaR* mutant compared to the *icaR* mutant. Interestingly, mutants A9, P4, D9, N2, and O7 had decreased *icaA* transcription when allelic replacement mutations in *icaR* and *tcaR* were introduced in this mutant background, suggesting that the function of IcaR and TcaR with regard to the regulation of *icaADBC* has been altered in these mutants. Unfortunately, for unknown reasons, we were unable to generate *tcaR* mutations in mutants A9 or P4 by either  $\Phi$ 71- and  $\Phi$ A6C-mediated transduction or direct allelic replacement methodologies.

Alongside CSF41498, we also isolated six 1457 mutants that made less PIA than did the wild type. Four were obtained using flow cell methodology, whereas 22R5 and 22R6 were isolated from a guinea pig tissue cage model (22, 80). With the exception of PV22, *icaA* transcription is markedly lower in these mutants compared to the 1457 wild-type strain, confirming that these mutants carry mutations that repress expression of *icaADBC*. In addition, other than strain 22R6, which appears to produce similar amounts of PIA as 1457, PIA immunoblot and biofilm assays corroborated this observation documenting that these isolates produce less PIA-mediated biofilm (Fig. 6). Importantly, other than strain PV22, all 1457 mutants had similar phenotypes as CSF41498. This phenotype included enhanced *icaR* transcript, decreased *icaA* transcript, and enhanced biofilm and PIA synthesis as well as an increase in *icaA* transcript when an *icaR* mutation was introduced. Other than a modest increase in PIA production, little phenotype was observed in the *tcaR* mutants. Interestingly, *icaA* transcription does not correlate with PIA synthesis and biofilm in mutant PV22; however, allelic replacement of *icaR* does result in increased PIA/biofilm synthesis. Collectively, these experiments with



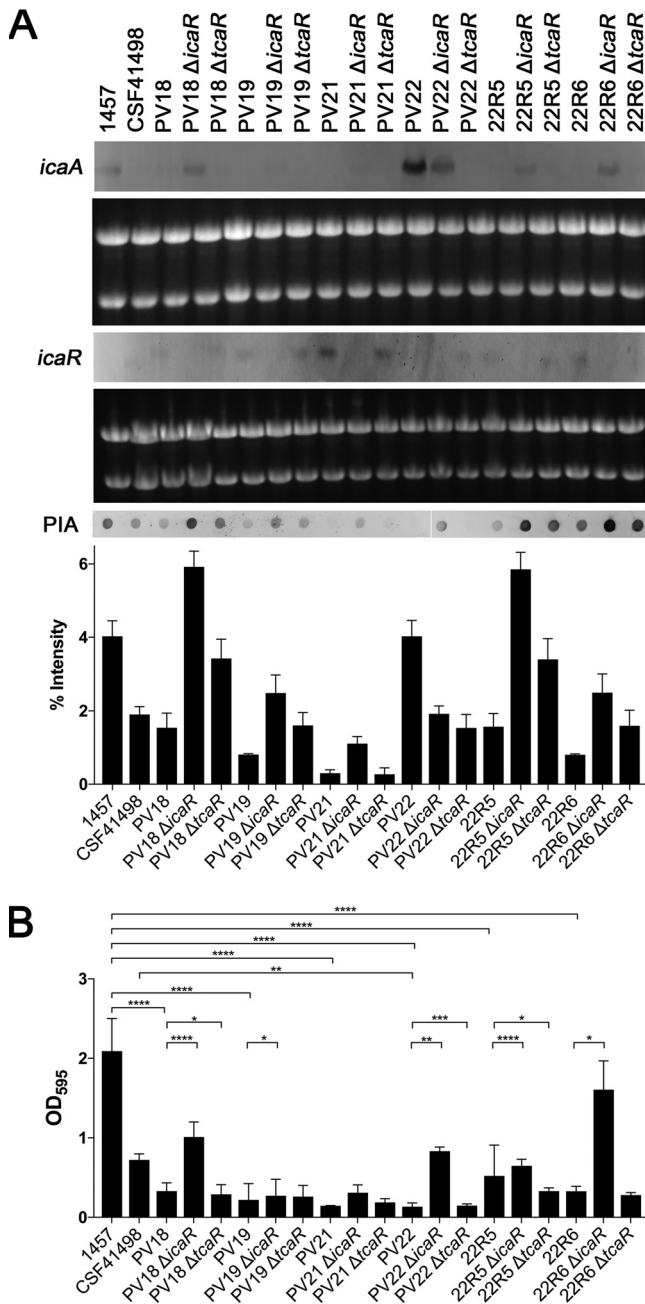


**FIG 6** *icaA* transcript, PIA synthesis, and biofilm production in 1457 mutants that produce less biofilm. (A and B) Northern blot analyses detecting *icaA* and *icaR* transcript in 1457 biofilm mutants in addition to PIA synthesis (A) and biofilm formation (B) compared to 1457 wild type (WT). Statistical analysis was performed using one-way ANOVA with Tukey's multiple-comparison test. \*,  $P \leq 0.05$ ; \*\*,  $P \leq 0.01$ ; \*\*\*,  $P \leq 0.001$ ; \*\*\*\*,  $P \leq 0.0001$ . An RNA gel is shown as a loading control. PIA dot blot and biofilm analyses were assessed from three biological replicates.

both CSF41498 and 1457 suggest that mutations can be easily selected that will result in decrease of *icaR* transcription, most likely yielding enhanced PIA synthesis. Further, compensatory mutations can also be easily selected from 1457 that facilitate the transcriptional regulation of *icaADBC* by IcaR, similar to the phenotype observed in CSF41498.

**Identification of mutations that facilitate altered PIA synthesis in 1457 and CSF41498.** Whole-genome sequencing was performed to identify mutations in the ten CSF41498 mutants and six 1457 mutants that were isolated. First, it is important to note that multiple mutations were detected in all strains sequenced (Table S3). In the 1457

mutants, we found mutations in several common genes, including ferrous iron transporter B (*feoB*), tributyrin esterase, phosphoenolpyruvate synthase regulatory protein, and RNase Y, as well as two hypothetical proteins with unknown function. Not surprisingly, we also discovered mutations in *icaA* (in PV22) and  $\sigma^B$  (PV19). As previously discussed,  $\sigma^B$  activates *icaADBC* by indirectly repressing *icaR* expression (64) therefore, mutations in either *icaA* or  $\sigma^B$  could lead to abolishment of *icaADBC* transcription and PIA synthesis.

Results from sequencing the ten CSF41498 mutants revealed that each carried mutations in multiple genes (Table S3). Some of the ten CSF41498 mutant isolates had mutated genes in common, including homoserine-*O*-acetyltransferase, aldehyde dehydrogenase A (*aldA*), *c*-di-AMP phosphodiesterase (*gdpP*), L-carnitine/choline transporter (*opuCA*), respiratory nitrate reductase (*narH*), and an Abr family transcriptional regulator. Unsurprisingly, we also discovered mutations in *icaB* and *icaR*. *icaB* is a deacetylase whose function is to impart a negative charge on PIA, allowing for interaction with the cell surface as well as to various surfaces. Surprisingly, a mutation in *icaB* was identified in mutant O7 which exhibits enhanced *icaA* transcription and PIA synthesis compared to the CSF41498 wild type (Fig. 5). These data may suggest that this substitution mutation in *icaB* results in enhanced IcaB activity, thus facilitating the phenotype observed in mutant O7. As expected, a mutation in *icaR* would lead to derepression of *icaADBC* and thus PIA synthesis and biofilm formation. Since these mutants all have mutations in multiple genes, it is likely that multiple mutations are required to alter *icaADBC* expression and PIA synthesis. Furthermore, many mutations are substitution mutations, and therefore the effects on protein function are largely unknown.

Aside from *icaR*, sequencing results identified one other transcriptional regulator potentially involved in regulation of *icaADBC*. In *B. subtilis*, AbrB regulates two genes implicated in biofilm formation: *yoaW* and *sipW*. SipW was shown to be a signal peptidase with function in processing either an intercellular adhesin or motility structure (81, 82). Considering this, the regulator we identified may also function to regulate biofilm formation in staphylococci. However, further experiments are required to confirm this.

Lastly, GGDEF domain-containing proteins have diguanylate cyclase activity (and sometimes phosphodiesterase activity) (83, 84). GdpS is the only staphylococcal protein carrying this highly conserved domain, whereas GdpP has a modified domain (85). GdpP has been shown to affect biofilm formation in several organisms (86–89), and GdpS can regulate PIA synthesis by increasing *icaADBC* mRNA levels (85). Since *gdpP* was mutated in multiple CSF41498 mutants, we speculated that GdpP can function to regulate *icaADBC* and PIA synthesis. To investigate whether inactivating *gdpP* would lead to decreased *icaADBC* transcription, *gdpP* mutants were generated in 1457 and CSF41498 using allelic replacement methodologies. We did not observe any change in *icaA* transcription or biofilm formation in the *gdpP* mutants of both 1457 and CSF41498 (Fig. S2), indicating that GdpP does not function alone in regulating PIA in *S. epidermidis*. While mutations in *gdpP* did arise in multiple CSF41498 biofilm mutants, it must be noted that these were substitution mutations. It is unknown what effects these substitutions have, if any, on protein function. Furthermore, the biofilm mutants carried mutations in multiple genes, suggesting that increased PIA synthesis could be due to a combination of multiple factors. Further studies are required to determine which of the remaining identified genes, or combination of genes, function in the regulation of PIA synthesis.

## DISCUSSION

*S. epidermidis* is a commensal skin bacterium common on a variety of sites, including the nares, axillae, arms, and legs (1). As part of the skin microbiota, *S. epidermidis* has been shown to play a protective role by preventing colonization of pathogens (2, 3). However, *S. epidermidis* is also known to cause various infections and is the most frequent cause of those involving indwelling medical devices, including catheters, cerebral spinal fluid shunts, and prosthetic joints (8). Unlike the abundance of virulence

factors that *S. aureus* possess, *S. epidermidis* has few virulence factors, and the most significant is the ability to form biofilm. While PIA has been shown to be an important component of biofilms, it is well known that not all *S. epidermidis* strains carry *icaADBC*, especially those isolated from healthy individuals (25, 43, 74, 90–93). Furthermore, previous studies have shown that *ica*-positive clinical isolates do not necessarily synthesize PIA, suggesting that *icaADBC* transcription is heavily repressed (36, 74). These data suggest that PIA synthesis, while important during biofilm formation and potentially during high shear stress, is not always advantageous. Indeed, our laboratory has previously demonstrated that, in a skin colonization model, an *ica* mutant was more adept at colonization of skin than a strain producing enhanced PIA (strain 1457). This, in combination with the observation that isolates from the skin of healthy individuals generally lack *icaADBC*, suggests that strains lacking this operon are selected for in this environment. It is possible that PIA masks molecules important for adherence to terminally differentiated keratinocytes. In addition, synthesis of PIA is expensive metabolically as carbon is shunted away from glycolysis and cell wall biosynthesis.

However, we propose that there may be niches where enhanced synthesis of PIA is selected. We have previously reported that *S. epidermidis* clinical isolates from a high-shear environment (such as catheters) are more likely to carry the *ica* operon and synthesize PIA than those from low-shear environments (74). Furthermore, *icaA* transcription and PIA synthesis are increased when biofilms are grown under high-shear flow (5, 49, 74). These data provide evidence that, while PIA is not advantageous under all conditions, there are circumstances under which strains able to synthesize PIA are selected. We studied here two *S. epidermidis* strains isolated from different infection sites that produce different PIA levels. 1457 was isolated from a catheter infection (high shear) and synthesizes high PIA and biofilm (94) while CSF41498 was isolated from a cerebral spinal fluid infection (low shear) and generally makes little PIA unless induced by NaCl (59). IcaR is a well-characterized repressor of *icaADBC* (59, 61, 63, 67, 68, 78); however, in contrast to CSF41498, an *icaR* mutation did not have any observable effects on *icaA* transcription or PIA synthesis in 1457. Less *icaR* transcript is detected in 1457 than in CSF41498, suggesting that *icaADBC* is derepressed in strain 1457 due to decreased *icaR* expression. Complementation of *icaR* using a constitutive promoter completely represses *icaA* transcription and PIA synthesis, demonstrating that IcaR is functional.

Furthermore, in 1457, where *icaR* transcription is reduced, TcaR was shown to be the primary repressor since a *tcaR* mutant results in significantly increased *icaA* transcription and PIA synthesis. However, in CSF41498, where IcaR is sufficient in repressing *icaADBC*, a *tcaR* mutant did not express *icaA*. These data confirm previous reports that TcaR is not a major repressor of *icaADBC* (63) and only function when the primary repressor, IcaR, is not present. This suggests that TcaR may have a lower binding affinity than IcaR. To investigate this, we performed DNase I footprinting and, indeed, were able to show that both IcaR and TcaR bound to the intergenic region between *icaR* and *icaA*. Although IcaR bound to one sequence near the *icaA* start site, TcaR bound to multiple sites, suggesting a possible binding competition between IcaR and TcaR. In addition, TcaR has binding sites in the *icaR* promoter, confirming transcriptional data that TcaR represses *icaR* transcription. This indicates that TcaR can function as a regulator of both *icaR* and *icaADBC*, providing multiple avenues by which TcaR can influence *icaADBC* transcription.

Our data thus far suggest that clinically relevant high PIA-producing strains, such as 1457, have gained mutations leading to decreased *icaR* expression and derepressed *icaADBC*. In an effort to identify these mutations, we sequenced 1457 mutants with decreased PIA synthesis and observed that, indeed, enhanced *icaR* transcription is detected. In addition, we identified a number of mutations that, perhaps cooperatively, could be responsible for repressing *icaR* transcription. Furthermore, we were able to easily isolate CSF41498 biofilm mutants displaying increased *icaA* transcription, PIA synthesis, and biofilm formation. Collectively, our results suggest that different mutations can be selected in *S. epidermidis* that

fine-tune PIA synthesis to allow for colonization in multiple niches of the host, including the epidermis and biomaterials.

## MATERIALS AND METHODS

**Culture media and growth conditions.** Bacterial strains and plasmids used in this study are listed in Table S1 in the supplemental material. *Escherichia coli* was grown in lysogeny broth (LB; Becton Dickinson Difco, Franklin Lakes, NJ), and staphylococcal strains were cultured using TSB (Becton Dickinson Difco). Antibiotics were used at the following concentrations: 10  $\mu\text{g/ml}$  chloramphenicol, 10  $\mu\text{g/ml}$  tetracycline, 10  $\mu\text{g/ml}$  trimethoprim, 10 to 50  $\mu\text{g/ml}$  erythromycin, and 100  $\mu\text{g/ml}$  kanamycin. These same concentrations were also used to grow *E. coli*, with the exception of kanamycin (50  $\mu\text{g/ml}$ ), erythromycin (500  $\mu\text{g/ml}$ ), and ampicillin (50  $\mu\text{g/ml}$ ). Cultures were grown aerobically (1:10 medium/flask ratio, 250 rpm) or microaerobically (3:5 medium/flask ratio, 125 rpm) at 37 or 30°C for temperature-sensitive strains.

**Generation of *tcaR* allelic replacement plasmid.** Primer pairs 2038-2039 (BamHI and XbaI) and 2015-2016 (Sall and PstI) (Table S2) were used to amplify the 5' and 3' regions, respectively, of *tcaR* using *S. epidermidis* 1457 as the template DNA (GenBank accession number CP020463.1). These sequences were inserted into the pUC19 multiple cloning site using the corresponding restriction enzyme sites. Primers 2234 and 2235 were used to amplify the *dhfr* cassette (conferring for trimethoprim resistance) and inserted between the 5' and 3' sequences using Sall and XbaI. PCR was performed with PfuI long-range DNA polymerase (Monserate Biotechnology Group, San Diego, CA). This construct was then digested with PstI and ligated into pROJ6448 to generate pNF263. pNF263 was isolated from *E. coli* DH5 $\alpha$  and electroporated into electrocompetent *S. aureus* RN4220 (95, 96). Plasmid DNA was then isolated from RN4220 and electroporated into electrocompetent *S. epidermidis* 1457 and transduced into CSF41498 via bacteriophage  $\Phi$ A6C.

**Generation of *icaR* and *tcaR* complementation strains.** The *sarA* promoter was amplified with 3090 and 3091 (*icaR*) or 3092 (*tcaR*), whereas the *icaR* and *tcaR* open reading frames were amplified with primer pairs 3093-2697 and 3094-3095, respectively (Table S2). Because these genes were driven by the constitutive *sarA* promoter instead of their native promoter, splicing with overlap extension (SOE) PCR was performed to ensure the *sarA* promoter could be cloned to the gene without introduction of restriction enzyme recognition sites. These sequences were ligated into pCL10 using KpnI and BamHI. The 5' and 3' regions of the lipase gene were amplified with primer pairs 3096-3097 (Sall and XbaI) and 3098-3099 (KpnI and SacI), respectively. A kanamycin resistance cassette was amplified with primers 3088 and 3089 and inserted between the 5' and 3' lipase sequences using BamHI and XbaI to generate pNF332 (*icaR*) and pNF333 (*tcaR*). These plasmids were constructed in *E. coli* DH5 $\alpha$ , electroporated into electrocompetent PS187  $\Delta$ *hdsR*  $\Delta$ *sauUSI*, before being transduced into *S. epidermidis* 1457 using bacteriophage  $\Phi$ 187 according to a previously described protocol (97, 98). A similar approach was used to generate the *gdpP* mutant using primers noted in Table S2.

**Allelic exchange.** *S. epidermidis* strains carrying the allelic replacement vectors were grown in TSB plus antibiotic (i.e., TSB plus erythromycin for pUC19-pROJ6448 or plus chloramphenicol for pCL10) at 30°C until to mid-exponential phase. This culture was then inoculated 1:100 into a fresh culture tube containing TSB only and grown at 45°C overnight. Cultures were diluted 1:100 in fresh TSB every day. Starting on the third day, cultures are serially diluted and plated on TSA plus antibiotic and grown at 45°C. These plates were then patched onto TSA plus antibiotic and confirmed as single recombinants by PCR. Single recombinants were inoculated into fresh culture tubes and grown as described above to generate double recombinants. To identify double recombinants, colonies were patched onto TSA plus mutant antibiotic marker (or just TSA if markerless mutant) and TSA plus vector antibiotic marker. Double recombinants were confirmed by PCR using primers located outside recombination region. When possible, mutations were backcrossed into a clean background using  $\Phi$ 71 or  $\Phi$ A6C (98).

**Transduction of  $\Delta$ *icaR* and  $\Delta$ *tcaR* mutants.** Mutations were transduced into clinical isolates and biofilm mutants with  $\Phi$ 71 or  $\Phi$ A6C propagated on 1457 *icaR::tetM* and 1457 *tcaR::dhfr*, as previously described (98).

**RNA isolation and Northern blot analyses.** Overnight cultures grown in TSB were diluted into flasks containing TSB to an optical density at 600 nm ( $\text{OD}_{600}$ ) of 0.05 and grown microaerobically. Cells were collected at the appropriate time points, pelleted at 4°C (5,000 rpm), and resuspended in 900  $\mu\text{l}$  of RLT buffer (Qiagen) (containing 10%  $\beta$ -mercaptoethanol). Cells were disrupted using a Bead Ruptor 24 (speed = 6.0, 25 s, two times; Omni International, Kennesaw, GA) and centrifuged at 13,000 rpm for 10 min at 4°C. The supernatant was added to 500  $\mu\text{l}$  of ethanol, and RNA was isolated using an RNeasy minikit according to the manufacturer's protocol (Qiagen, Hilden, Germany). Next, 4 to 5  $\mu\text{g}$  of RNA was subjected to Northern blot analyses using DNA probes amplified with digoxigenin (DIG)-labeled dUTP (primers listed in Table S2; Roche, Indianapolis, IN). Probe detection was performed with antidigoxigenin-alkaline phosphatase (AP) Fab fragments (Roche) and ECF substrate (GE Healthcare) or CDP Star chemiluminescent substrate (Life Technologies, Bedford, MA). Each Northern blot analysis was performed at least three independent times.

**Quantitative real-time PCR.** cDNA was generated using a QuantiTect reverse transcription kit (Qiagen) with  $\sim$ 500 ng of RNA/sample. qRT-PCR was performed with a LightCycler 480 SYBR green I Master kit (Roche) using cDNA (diluted 1:20) from *S. epidermidis* strains using a LightCycler 480 II instrument (Roche). *tcaR* and *icaA* transcript levels were normalized to *gyrB* and are reported as the fold change compared to wild-type levels.

**PIA immunoblot assay.** Bacterial cultures were collected to an adjusted  $\text{OD}_{600}$  of 5 and pelleted by centrifugation (5,000 rpm, 5 min). PIA was isolated as previously described (99). Briefly, pellets were

resuspended in 500  $\mu$ l of TE buffer and heated at 100°C for 5 min. The samples were centrifuged; the supernatants were separated and treated with proteinase K for 1 h at 37°C and then heated at 95°C for 10 min to inactivate the proteinase K. PIA preparations were applied to 0.45- $\mu$ m nitrocellulose membranes (Bio-Rad Laboratories) using a Bio-Dot apparatus (Bio-Rad Laboratories), and Western blot analyses were performed with rabbit anti-PIA primary antibody (a gift from Jim O'Gara, National University of Ireland, Galway, Ireland) and AP-conjugated goat anti-rabbit secondary antibody (Jackson ImmunoResearch, West Grove, PA). Detection and visualization were completed using ECF chemiluminescent substrate (GE Healthcare Life Sciences) and a Typhoon FLA 7000 (GE Healthcare Life Sciences).

**Static biofilm assay.** Christensen biofilm assays were performed as previously described (79, 100). Briefly, cultures were grown in TSB in 96-well flat-bottom Delta Surface plates (Corning). After overnight incubation in a 37°C static incubator, the plates were washed with phosphate-buffered saline (PBS), dried (inverted) at 45°C for 2 h, and then stained with 150  $\mu$ l of crystal violet stain for 15 min at room temperature. After removal of the stain, the plates were washed under running water until the water ran colorless. Crystal violet stain was solubilized with 95% ethanol for more consistent quantification on a plate reader (OD<sub>595</sub>).

**Recombinant protein purification.** The open reading frames of *icaR* and *tcaR* were PCR amplified with primer pairs 2692-2357 and 2358-2359 (respectively) using Pfu<sup>+</sup> long-range DNA polymerase (Monserate Biotechnology Group) and cloned into the protein expression vector pET15b or pET28a using the BamHI and NdeI sites. These expression vectors were expressed in the *E. coli* protein expressing strains BL21(DE3) (IcaR) or Arctic Express (TcaR). IcaR was induced using autoinduction medium (adapted from reference 101) for 18 h at 37°C aerobically. To induce TcaR, Arctic Express pNF352 was grown in LB plus ampicillin aerobically to an OD<sub>600</sub> of 0.6 and then induced with 1 mM IPTG (isopropyl- $\beta$ -D-thiogalactopyranoside) for 3 h. Induced cultures were pelleted at 4°C and resuspended in equilibrium buffer (1:20) containing protease inhibitors (4 mM phenylmethylsulfonyl fluoride, 1 mM N-ethylmaleimide [NEM], 25 mM 6-aminohexanoic acid [EACA]). Cells were passaged through an Emulsiflex C3 (Avestin, Ottawa, Ontario, Canada) three times to lyse cells. Samples were then centrifuged at 4°C, and supernatants were incubated with 1 ml of HisPur cobalt resin (Pierce Biotechnology, Rockford, IL) overnight on an end-over-end mixer at 4°C. Resin was then washed and eluted according to the manufacturer's instructions. Purified proteins were concentrated at 20°C using a Vivaspin 10,000-molecular-weight-cutoff (MWCO) column (Sartorius AG, Göttingen, Germany) and stored in PBS with 30% glycerol at -20°C.

**Electrophoretic mobility shift assay.** Primers 2850 and 2851 were used to amplify the *ica* promoter carrying a fluorescein tag. Increasing concentrations (100 to 1,000 pmol) of recombinant IcaR and TcaR were incubated with fluorescein-labeled DNA in binding buffer (20 mM Tris-HCl [pH 8.0], 150 mM KCl, 0.1 mM MgCl<sub>2</sub>, 0.05 mM EDTA, 12.5% glycerol, 10 mM dithiothreitol [DTT], 1 mg/ml bovine serum albumin [BSA]) for 30 min at room temperature. Next, 10  $\mu$ l of 10 mg/ml salmon sperm DNA was added as noncompetitive DNA. Then, 15.8  $\mu$ M unlabeled DNA (amplified with primers 2865 and 2851) was added as competitive DNA. After incubation, loading buffer was added to each reaction mixture and loaded onto a 6% polyacrylamide gel (0.5 $\times$  Tris-borate-EDTA [TBE], 0.2% glycerol, 6% bisacrylamide, TEMED, APS). Samples were electrophoresed in 0.5 $\times$  TBE and visualized on a Typhoon FLA 7000 (GE Healthcare).

**Generation of <sup>32</sup>P-labeled DNA.** Primer 2855 was labeled with <sup>32</sup>P by incubation with 10 $\times$  kinase buffer, T4 polynucleotide kinase, and [<sup>32</sup>P]ATP for 30 min at 37°C. The primer was then precipitated with ammonium acetate, glycogen, and ice-cold ethanol in dry ice for 10 min, followed by pelleting by centrifugation and a wash with cold 70% ethanol. A SpeedVac concentrator (Thermo Scientific) attached to a vacuum pump was used to dry the pelleted, labeled primer.

The *icaR-icaA* intergenic region was amplified with labeled primer 2855 and unlabeled primer 2965 using HiFi Platinum *Taq* polymerase (Invitrogen, Carlsbad, CA) with 1457 genomic DNA as the template. Labeled PCR product was cleaned using Wizard SV gel and a PCR Clean-Up system (Promega, Madison, WI).

**DNase I footprinting assay.** Labeled DNA was incubated with recombinant IcaR or TcaR in binding buffer (20 mM Tris-HCl [pH 8.0], 150 mM KCl, 0.1 mM MgCl<sub>2</sub>, 0.05 mM EDTA, 12.5% glycerol, 10 mM DTT, 1 mg/ml BSA), to a final volume of 20  $\mu$ l for 15 min at room temperature. Then, 20  $\mu$ l of 5 mM CaCl<sub>2</sub>-10 mM MgCl<sub>2</sub> was added to each reaction, followed by 10  $\mu$ l of diluted DNase I. Next, 100  $\mu$ l of STOP buffer (0.125% SDS, 12.5 mM EDTA, 3 mg/ml glycogen) was added exactly 1 min after the addition of DNase I, and the reaction mixture was placed on ice. A 100- $\mu$ l portion of phenol-chloroform-isoamyl alcohol (25:24:1) was added, and the reaction mixture was mixed by flicking, followed by centrifugation to separate the layers. The aqueous layer was moved to a new tube containing 1 ml of ice cold ethanol and stored at -20°C overnight (or on dry ice for 15 min). The DNA was pelleted by centrifugation for 20 min, the ethanol was removed, and the pellet was washed with 70% ethanol. A SpeedVac concentrator (Fisher Scientific) was used to dry the pellet. The pellet was then resuspended in 7  $\mu$ l of loading buffer (7 M urea, 0.1 $\times$  TBE, 0.05% bromophenol blue, 0.05% xylene cyanol FF), heated at 95°C for 2 min in a thermal cycler, and loaded onto a 6% denaturing polyacrylamide gel (42% urea, 1 $\times$  TBE, 6% polyacrylamide, TEMED, APS). The gel was electrophoresed on a prewarmed (50°C) Sequi-Gen GT nucleic acid electrophoresis cell (Bio-Rad) apparatus at 50 W in 0.5 $\times$  TBE until the dye front migrates  $\frac{3}{4}$  of the way through the gel, maintaining buffer temperature at 50 to 55°C. The gel was then transferred onto a large piece of Whatman paper (GE Healthcare), covered in plastic wrap, and dried on a gel dryer attached to a vacuum pump. Finally, the dried gel was developed using autoradiography film.

**Isolation of biofilm mutants.** Polystyrene tissue culture flasks (25 cm<sup>2</sup>; Corning Life Sciences, Durham, NC) were filled with 5 ml of TSB and inoculated with a single colony of *S. epidermidis* CSF41498. The flask was stored in a 37°C static incubator, with washing and replacement with fresh TSB media every day. On day 5, the flasks were washed with sterile saline, and the biofilm was removed from the flask

surface using a cell scraper (Biologix Corp, Shandong, China). The biofilms were dispersed using a sonic dismembrator (Fisher Scientific) on setting 1, serial diluted, and plated on Congo red agar (79).

**Generation of 1457 biofilm mutants.** Stovall convertible flow cells (24 mm by 40 mm by 8 mm; Stovall, Greensboro, NC) were filled with sterile TSB and inoculated with overnight cultures of *S. epidermidis* 1457. Biofilms were grown at 37°C at a flow rate of 0.5 ml/min for 24 h.

**DNA sequencing of biofilm mutants.** Isolates were sequenced on a MiSeq short-read sequencing platform (Illumina, Inc.) which produced reads with an average length of 300 bp and insert size of 500 bp, as previously described (102) at the Multidrug-Resistant Organism Repository and Surveillance Network (MRSN) of WRAIR. These reads were mapped to the complete CSF41498 genome (GenBank accession numbers CP030246 to CP030249); single nucleotide polymorphisms (SNPs) were then identified using Geneious software (Biomatters, New Zealand) based on CSF41498 annotation. All SNPs found had a read frequency of >0.9. The 13-kb deletion was identified as present in a mixed population by a read coverage of less than half the genome average.

## SUPPLEMENTAL MATERIAL

Supplemental material for this article may be found at <https://doi.org/10.1128/JB.00524-18>.

**SUPPLEMENTAL FILE 1**, PDF file, 0.7 MB.

## ACKNOWLEDGMENT

This study was funded by NIH/NIAID P01 AI083211 (P.D.F.).

## REFERENCES

- Kloos WE, Musselwhite MS. 1975. Distribution and persistence of *Staphylococcus* and *Micrococcus* species and other aerobic bacteria on human skin. *Appl Microbiol* 30:381–385.
- Cogen A, Nizet V, Gallo R. 2007. *Staphylococcus epidermidis* functions as a component of the skin innate immune system by inhibiting the pathogen group A streptococcus. *J Invest Dermatol* 127:S131–S131.
- Cogen AL, Nizet V, Gallo RL. 2008. Skin microbiota: a source of disease or defence? *Br J Dermatol* 158:442–455. <https://doi.org/10.1111/j.1365-2133.2008.08437.x>.
- Naik S, Bouladoux N, Linehan JL, Han SJ, Harrison OJ, Wilhelm C, Conlan S, Himmelfarb S, Byrd AL, Deming C, Quinones M, Brenchley JM, Kong HH, Tussiwand R, Murphy KM, Merad M, Segre JA, Belkaid Y. 2015. Commensal-dendritic-cell interaction specifies a unique protective skin immune signature. *Nature* 520:104–108. <https://doi.org/10.1038/nature14052>.
- Weaver WM, Milisavljevic V, Miller JF, Di Carlo D. 2012. Fluid flow induces biofilm formation in *Staphylococcus epidermidis* polysaccharide intracellular adhesion-positive clinical isolates. *Appl Environ Microbiol* 78:5890–5896. <https://doi.org/10.1128/AEM.01139-12>.
- Zimmerli W, Trampuz A, Ochsner PE. 2004. Prosthetic-joint infections. *N Engl J Med* 351:1645–1654. <https://doi.org/10.1056/NEJMra040181>.
- National Nosocomial Infections Surveillance Survey. 2004. National Nosocomial Infections Surveillance (NNIS) System Report, data summary from January 1992 through June 2004, issued October 2004. *Am J Infect Control* 32:470–485.
- Rogers KL, Fey PD, Rupp ME. 2009. Coagulase-negative staphylococcal infections. *Infect Dis Clin North America* 23:73–98. <https://doi.org/10.1016/j.idc.2008.10.001>.
- Weiner LM, Webb AK, Limbago B, Dudeck MA, Patel J, Kallen AJ, Edwards JR, Sievert DM. 2016. Antimicrobial-resistant pathogens associated with healthcare-associated infections: summary of data reported to the National Healthcare Safety Network at the Centers for Disease Control and Prevention, 2011–2014. *Infect Control Hosp Epidemiol* 37:1288–1301. <https://doi.org/10.1017/ice.2016.174>.
- von Eiff C, Peters G, Heilmann C. 2002. Pathogenesis of infections due to coagulase-negative staphylococci. *Lancet Infect Dis* 2:677–685.
- Cue D, Lei MG, Lee CY. 2012. Genetic regulation of the intercellular adhesion locus in staphylococci. *Front Cell Infect Microbiol* 2:38. <https://doi.org/10.3389/fcimb.2012.00038>.
- Otto M. 2009. *Staphylococcus epidermidis*: the “accidental” pathogen. *Nat Rev Microbiol* 7:555–567. <https://doi.org/10.1038/nrmicro2182>.
- Anderl JN, Franklin MJ, Stewart PS. 2000. Role of antibiotic penetration limitation in *Klebsiella pneumoniae* biofilm resistance to ampicillin and ciprofloxacin. *Antimicrob Agents Chemother* 44:1818–1824.
- Gagnon RF, Richards GK, Wiesenfeld L. 1991. *Staphylococcus epidermidis* biofilms: unexpected outcome of double and triple antibiotic combinations with rifampin. *ASAIO Trans* 37:M158–M160.
- Yao Y, Sturdevant DE, Otto M. 2005. Genomewide analysis of gene expression in *Staphylococcus epidermidis* biofilms: insights into the pathophysiology of *S. epidermidis* biofilms and the role of phenol-soluble modulins in formation of biofilms. *J Infect Dis* 191:289–298. <https://doi.org/10.1086/426945>.
- Paharik AE, Horswill AR. 2016. The staphylococcal biofilm: adhesins, regulation, and host response. *Microbiol Spectr* 4(2):microbiolspec.VMBF-0022-2015. <https://doi.org/10.1128/microbiolspec.VMBF-0022-2015>.
- Moormeier DE, Bose JL, Horswill AR, Bayles KW. 2014. Temporal and stochastic control of *Staphylococcus aureus* biofilm development. *mBio* 5:e01341-14. <https://doi.org/10.1128/mBio.01341-14>.
- Holland LM, Conlon B, O’Gara JP. 2011. Mutation of *tagO* reveals an essential role for wall teichoic acids in *Staphylococcus epidermidis* biofilm development. *Microbiology* 157:408–418. <https://doi.org/10.1099/mic.0.042234-0>.
- Gross M, Cramton SE, Gotz F, Peschel A. 2001. Key role of teichoic acid net charge in *Staphylococcus aureus* colonization of artificial surfaces. *Infect Immun* 69:3423–3426. <https://doi.org/10.1128/IAI.69.5.3423-3426.2001>.
- Kiedrowski MR, Kavanaugh JS, Malone CL, Mootz JM, Voyich JM, Smeltzer MS, Bayles KW, Horswill AR. 2011. Nuclease modulates biofilm formation in community-associated methicillin-resistant *Staphylococcus aureus*. *PLoS One* 6:e26714. <https://doi.org/10.1371/journal.pone.0026714>.
- Izano EA, Amarante MA, Kher WB, Kaplan JB. 2008. Differential roles of poly-N-acetylglucosamine surface polysaccharide and extracellular DNA in *Staphylococcus aureus* and *Staphylococcus epidermidis* biofilms. *Appl Environ Microbiol* 74:470–476. <https://doi.org/10.1128/AEM.02073-07>.
- Fey PD, Olson ME. 2010. Current concepts in biofilm formation of *Staphylococcus epidermidis*. *Future Microbiol* 5:917–933. <https://doi.org/10.2217/fmb.10.56>.
- Montanaro L, Poggi A, Visai L, Ravaioli S, Campoccia D, Speziale P, Arciola CR. 2011. Extracellular DNA in biofilms. *Int J Artif Organs* 34:824–831. <https://doi.org/10.5301/ijao.5000051>.
- Mann EE, Rice KC, Boles BR, Endres JL, Ranjit D, Chandramohan L, Tsang LH, Smeltzer MS, Horswill AR, Bayles KW. 2009. Modulation of eDNA release and degradation affects *Staphylococcus aureus* biofilm maturation. *PLoS One* 4:e5822. <https://doi.org/10.1371/journal.pone.0005822>.
- Cafiso V, Bertuccio T, Santagati M, Campanile F, Amicosante G, Perilli MG, Selan L, Artini M, Nicoletti G, Stefani S. 2004. Presence of the *ica* operon in clinical isolates of *Staphylococcus epidermidis* and its role in biofilm production. *Clin Microbiol Infect* 10:1081–1088. <https://doi.org/10.1111/j.1469-0691.2004.01024.x>.
- Cramton SE, Gerke C, Schnell NF, Nichols WW, Gotz F. 1999. The

- intercellular adhesion (*ica*) locus is present in *Staphylococcus aureus* and is required for biofilm formation. *Infect Immun* 67:5427–5433.
27. Gerke C, Kraft A, Sussmuth R, Schweitzer O, Gotz F. 1998. Characterization of the *N*-acetylglucosaminyltransferase activity involved in the biosynthesis of the *Staphylococcus epidermidis* polysaccharide intercellular adhesin. *J Biol Chem* 273:18586–18593.
  28. Heilmann C, Schweitzer O, Gerke C, Vanittanakom N, Mack D, Gotz F. 1996. Molecular basis of intercellular adhesion in the biofilm-forming *Staphylococcus epidermidis*. *Mol Microbiol* 20:1083–1091.
  29. Li H, Xu L, Wang J, Wen Y, Vuong C, Otto M, Gao Q. 2005. Conversion of *Staphylococcus epidermidis* strains from commensal to invasive by expression of the *ica* locus encoding production of biofilm exopolysaccharide. *Infect Immun* 73:3188–3191. <https://doi.org/10.1128/IAI.73.5.3188-3191.2005>.
  30. Little DJ, Bamford NC, Pokrovskaya V, Robinson H, Nitz M, Howell PL. 2014. Structural basis for the inter-cellular adhesion of poly- $\beta$ -1,6-*N*-acetyl-D-glucosamine in Gram-positive bacteria. *J Biol Chem* 289:35907–35917. <https://doi.org/10.1074/jbc.M114.611400>.
  31. Mack D, Fischer W, Krokotsch A, Leopold K, Hartmann R, Egge H, Laufs R. 1996. The intercellular adhesion involved in biofilm accumulation of *Staphylococcus epidermidis* is a linear  $\beta$ -1,6-linked glucosaminoglycan: purification and structural analysis. *J Bacteriol* 178:175–183.
  32. Mack D, Haeder M, Siemssen N, Laufs R. 1996. Association of biofilm production of coagulase-negative staphylococci with expression of a specific polysaccharide intercellular adhesin. *J Infect Dis* 174:881–884.
  33. McKenney D, Hubner J, Muller E, Wang Y, Goldmann DA, Pier GB. 1998. The *ica* locus of *Staphylococcus epidermidis* encodes production of the capsular polysaccharide/adhesin. *Infect Immun* 66:4711–4720.
  34. O'Gara JP. 2007. *ica* and beyond: biofilm mechanisms and regulation in *Staphylococcus epidermidis* and *Staphylococcus aureus*. *FEMS Microbiol Lett* 270:179–188. <https://doi.org/10.1111/j.1574-6968.2007.00688.x>.
  35. Olson ME, Garvin KL, Fey PD, Rupp ME. 2006. Adherence of *Staphylococcus epidermidis* to biomaterials is augmented by PIA. *Clin Orthop Relat Res* 451:21–24. <https://doi.org/10.1097/01.blo.0000229320.45416.0c>.
  36. Rohde H, Burandt EC, Siemssen N, Frommelt L, Burdelski C, Wurster S, Scherpe S, Davies AP, Harris LG, Horstkotte MA, Knobloch JK, Ragunath C, Kaplan JB, Mack D. 2007. Polysaccharide intercellular adhesion or protein factors in biofilm accumulation of *Staphylococcus epidermidis* and *Staphylococcus aureus* isolated from prosthetic hip and knee joint infections. *Biomaterials* 28:1711–1720. <https://doi.org/10.1016/j.biomaterials.2006.11.046>.
  37. Rupp ME, Fey PD, Heilmann C, Gotz F. 2001. Characterization of the importance of *Staphylococcus epidermidis* autolysin and polysaccharide intercellular adhesin in the pathogenesis of intravascular catheter-associated infection in a rat model. *J Infect Dis* 183:1038–1042. <https://doi.org/10.1086/319279>.
  38. Rupp ME, Ulphani JS, Fey PD, Bartscht K, Mack D. 1999. Characterization of the importance of polysaccharide intercellular adhesin/hemagglutinin of *Staphylococcus epidermidis* in the pathogenesis of biomaterial-based infection in a mouse foreign body infection model. *Infect Immun* 67:2627–2632.
  39. Rupp ME, Ulphani JS, Fey PD, Mack D. 1999. Characterization of *Staphylococcus epidermidis* polysaccharide intercellular adhesin/hemagglutinin in the pathogenesis of intravascular catheter-associated infection in a rat model. *Infect Immun* 67:2656–2659.
  40. Vuong C, Kidder JB, Jacobson ER, Otto M, Proctor RA, Somerville GA. 2005. *Staphylococcus epidermidis* polysaccharide intercellular adhesion production significantly increases during tricarboxylic acid cycle stress. *J Bacteriol* 187:2967–2973. <https://doi.org/10.1128/JB.187.9.2967-2973.2005>.
  41. Vuong C, Voyich JM, Fischer ER, Braughton KR, Whitney AR, DeLeo FR, Otto M. 2004. Polysaccharide intercellular adhesin (PIA) protects *Staphylococcus epidermidis* against major components of the human innate immune system. *Cell Microbiol* 6:269–275.
  42. Yakandawala N, Gawande PV, LoVetri K, Cardona ST, Romeo T, Nitz M, Madhyastha S. 2011. Characterization of the poly- $\beta$ -1,6-*N*-acetylglucosamine polysaccharide component of *Burkholderia* biofilms. *Appl Environ Microbiol* 77:8303–8309. <https://doi.org/10.1128/AEM.05814-11>.
  43. Ziebuhr W, Heilmann C, Gotz F, Meyer P, Wilms K, Straube E, Hacker J. 1997. Detection of the intercellular adhesion gene cluster (*ica*) and phase variation in *Staphylococcus epidermidis* blood culture strains and mucosal isolates. *Infect Immun* 65:890–896.
  44. Cucarella C, Solano C, Valle J, Amorena B, Lasa I, Penades JR. 2001. Bap, a *Staphylococcus aureus* surface protein involved in biofilm formation. *J Bacteriol* 183:2888–2896. <https://doi.org/10.1128/JB.183.9.2888-2896.2001>.
  45. Hussain M, Herrmann M, von Eiff C, Perdreau-Remington F, Peters G. 1997. A 140-kilodalton extracellular protein is essential for the accumulation of *Staphylococcus epidermidis* strains on surfaces. *Infect Immun* 65:519–524.
  46. Rohde H, Burdelski C, Bartscht K, Hussain M, Buck F, Horstkotte MA, Knobloch JK, Heilmann C, Herrmann M, Mack D. 2005. Induction of *Staphylococcus epidermidis* biofilm formation via proteolytic processing of the accumulation-associated protein by staphylococcal and host proteases. *Mol Microbiol* 55:1883–1895. <https://doi.org/10.1111/j.1365-2958.2005.04515.x>.
  47. Christner M, Franke GC, Schommer NN, Wendt U, Wegert K, Pehle P, Kroll G, Schulze C, Buck F, Mack D, Aepfelbacher M, Rohde H. 2010. The giant extracellular matrix-binding protein of *Staphylococcus epidermidis* mediates biofilm accumulation and attachment to fibronectin. *Mol Microbiol* 75:187–207. <https://doi.org/10.1111/j.1365-2958.2009.06981.x>.
  48. Schaeffer CR, Woods KM, Longo GM, Kiedrowski MR, Paharik AE, Buttner H, Christner M, Boissy RJ, Horswill AR, Rohde H, Fey PD. 2015. Accumulation-associated protein enhances *Staphylococcus epidermidis* biofilm formation under dynamic conditions and is required for infection in a rat catheter model. *Infect Immun* 83:214–226. <https://doi.org/10.1128/IAI.02177-14>.
  49. Foka A, Katsikogianni MG, Anastassiou ED, Spiliopoulou I, Missirlis YF. 2012. The combined effect of surface chemistry and flow conditions on *Staphylococcus epidermidis* adhesion and *ica* operon expression. *Eur Cell Mater* 24:386–402.
  50. Mertens A, Ghebremedhin B. 2013. Genetic determinants and biofilm formation of clinical *Staphylococcus epidermidis* isolates from blood cultures and indwelling devices. *Eur J Microbiol Immunol* 3:111–119. <https://doi.org/10.1556/EuJMI.3.2013.2.4>.
  51. Harris LG, Murray S, Pascoe B, Bray J, Meric G, Mageiros L, Wilkinson TS, Jeeves R, Rohde H, Schwarz S, de Lencastre H, Miragaia M, Rolo J, Bowden R, Jolley KA, Maiden MC, Mack D, Sheppard SK. 2016. Biofilm morphotypes and population structure among *Staphylococcus epidermidis* from commensal and clinical samples. *PLoS One* 11:e0151240. <https://doi.org/10.1371/journal.pone.0151240>.
  52. Mekni MA, Bouchami O, Achour W, Ben Hassen A. 2012. Strong biofilm production but not adhesion virulence factors can discriminate between invasive and commensal *Staphylococcus epidermidis* strains. *APMIS* 120:605–611. <https://doi.org/10.1111/j.1600-0463.2012.02877.x>.
  53. Diemond-Hernández B, Solórzano-Santos, Leños-Miranda B, Peregrino-Bejarano L, Miranda-Novales G. 2010. Production of *icaADBC*-encoded polysaccharide intercellular adhesin and therapeutic failure in pediatric patients with staphylococcal device-related infections. *BMC Infect Dis* 10:68. <https://doi.org/10.1186/1471-2334-10-68>.
  54. Petrelli D, Zampaloni C, D'Ercole S, Prenna M, Ballarini P, Ripa S, Vitali LA. 2006. Analysis of different genetic traits and their association with biofilm formation in *Staphylococcus epidermidis* isolates from central venous catheter infections. *Eur J Clin Microbiol Infect Dis* 25:773–781. <https://doi.org/10.1007/s10096-006-0226-8>.
  55. Rohde H, Kalitzky M, Kroger N, Scherpe S, Horstkotte MA, Knobloch JK, Zander AR, Mack D. 2004. Detection of virulence-associated genes not useful for discriminating between invasive and commensal *Staphylococcus epidermidis* strains from a bone marrow transplant unit. *J Clin Microbiol* 42:5614–5619. <https://doi.org/10.1128/JCM.42.12.5614-5619.2004>.
  56. Heilmann C, Gerke C, Perdreau-Remington F, Götz F. 1996. Characterization of Tn917 insertion mutants of *Staphylococcus epidermidis* affected in biofilm formation. *Infect Immun* 64:277–282.
  57. Mack D, Nedelmann M, Krokotsch A, Schwarzkopf A, Heesemann J, Laufs R. 1994. Characterization of transposon mutants of biofilm-producing *Staphylococcus epidermidis* impaired in the accumulative phase of biofilm production: genetic identification of a hexosamine-containing polysaccharide intercellular adhesin. *Infect Immun* 62:3244–3253.
  58. Heilmann C, Gotz F. 1998. Further characterization of *Staphylococcus epidermidis* transposon mutants deficient in primary attachment or intercellular adhesion. *Zentralbl Bakteriol* 287:69–83.
  59. Conlon KM, Humphreys H, O'Gara JP. 2002. *icaR* encodes a transcriptional repressor involved in environmental regulation of *ica* operon expression and biofilm formation in *Staphylococcus epidermidis*. *J*

- Bacteriol 184:4400–4408. <https://doi.org/10.1128/JB.184.16.4400-4408.2002>.
60. Knobloch JK, Bartscht K, Sabottke A, Rohde H, Feucht HH, Mack D. 2001. Biofilm formation by *Staphylococcus epidermidis* depends on functional RsbU, an activator of the sigB operon: differential activation mechanisms due to ethanol and salt stress. *J Bacteriol* 183:2624–2633. <https://doi.org/10.1128/JB.183.8.2624-2633.2001>.
  61. Cerca N, Brooks JL, Jefferson KK. 2008. Regulation of the intercellular adhesin locus regulator (*icaR*) by SarA,  $\sigma^B$ , and IcaR in *Staphylococcus aureus*. *J Bacteriol* 190:6530–6533. <https://doi.org/10.1128/JB.00482-08>.
  62. Jager S, Jonas B, Pfanzelt D, Horstkotte MA, Rohde H, Mack D, Knobloch JK. 2009. Regulation of biofilm formation by  $\sigma^B$  is a common mechanism in *Staphylococcus epidermidis* and is not mediated by transcriptional regulation of *sarA*. *Int J Artif Organs* 32:584–591.
  63. Jefferson KK, Pier DB, Goldmann DA, Pier GB. 2004. The teicoplanin-associated locus regulator (TcaR) and the intercellular adhesin locus regulator (IcaR) are transcriptional inhibitors of the *ica* locus in *Staphylococcus aureus*. *J Bacteriol* 186:2449–2456. <https://doi.org/10.1128/JB.186.8.2449-2456.2004>.
  64. Knobloch JK, Jager S, Horstkotte MA, Rohde H, Mack D. 2004. RsbU-dependent regulation of *Staphylococcus epidermidis* biofilm formation is mediated via the alternative sigma factor  $\sigma^B$  by repression of the negative regulator gene *icaR*. *Infect Immun* 72:3838–3848. <https://doi.org/10.1128/IAI.72.7.3838-3848.2004>.
  65. Tormo MA, Marti M, Valle J, Manna AC, Cheung AL, Lasa I, Penades JR. 2005. SarA is an essential positive regulator of *Staphylococcus epidermidis* biofilm development. *J Bacteriol* 187:2348–2356. <https://doi.org/10.1128/JB.187.7.2348-2356.2005>.
  66. Handke LD, Slater SR, Conlon KM, O'Donnell ST, Olson ME, Bryant KA, Rupp ME, O'Gara JP, Fey PD. 2007.  $\sigma^B$  and SarA independently regulate polysaccharide intercellular adhesin production in *Staphylococcus epidermidis*. *Can J Microbiol* 53:82–91. <https://doi.org/10.1139/w06-108>.
  67. Jeng WY, Ko TP, Liu CL, Guo RT, Liu CL, Shr HL, Wang AH. 2008. Crystal structure of IcaR, a repressor of the TetR family implicated in biofilm formation in *Staphylococcus epidermidis*. *Nucleic Acids Res* 36:1567–1577. <https://doi.org/10.1093/nar/gkm1176>.
  68. Conlon KM, Humphreys H, O'Gara JP. 2002. Regulation of *icaR* gene expression in *Staphylococcus epidermidis*. *FEMS Microbiol Lett* 216:171–177. <https://doi.org/10.1111/j.1574-6968.2002.tb11432.x>.
  69. Brandenberger M, Tschierske M, Giachino P, Wada A, Berger BB. 2000. Inactivation of a novel three-cistronic operon *tcaR-tcaA-tcaB* increases teicoplanin resistance in *Staphylococcus aureus*. *Biochim Biophys Acta* 1523:135–139.
  70. McCallum N, Bischoff M, Maki H, Wada A, Berger BB. 2004. TcaR, a putative MarR-like regulator of *sarS* expression. *J Bacteriol* 186:2966–2972.
  71. Tegmark K, Karlsson A, Arvidson S. 2000. Identification and characterization of SarH1, a new global regulator of virulence gene expression in *Staphylococcus aureus*. *Mol Microbiol* 37:398–409.
  72. Chang YM, Jeng WY, Ko TP, Yeh YJ, Chen CK, Wang AH. 2010. Structural study of TcaR and its complexes with multiple antibiotics from *Staphylococcus epidermidis*. *Proc Natl Acad Sci U S A* 107:8617–8622. <https://doi.org/10.1073/pnas.0913302107>.
  73. Fan JR, Zhang HX, Mu YG, Zheng QC. 2018. Studying the recognition mechanism of TcaR and ssDNA using molecular dynamic simulations. *J Mol Graph Model* 80:67–75. <https://doi.org/10.1016/j.jmgm.2017.12.001>.
  74. Schaeffer CR, Hoang TN, Sudbeck CM, Alawi M, Tolo IE, Robinson DA, Horswill AR, Rohde H, Fey PD. 2016. Versatility of biofilm matrix molecules in *Staphylococcus epidermidis* clinical isolates and importance of polysaccharide intercellular adhesin expression during high shear stress. *mSphere* 1:e00165-16. <https://doi.org/10.1128/mSphere.00165-16>.
  75. Eftekhari F, Speert DP. 2009. Biofilm formation by persistent and non-persistent isolates of *Staphylococcus epidermidis* from a neonatal intensive care unit. *J Hosp Infect* 71:112–116. <https://doi.org/10.1016/j.jhin.2008.09.008>.
  76. Chokr A, Watier D, Eleaume H, Pangon B, Ghnassia JC, Mack D, Jabbouri S. 2006. Correlation between biofilm formation and production of polysaccharide intercellular adhesin in clinical isolates of coagulase-negative staphylococci. *Int J Med Microbiol* 296:381–388. <https://doi.org/10.1016/j.ijmm.2006.02.018>.
  77. Ballal A, Manna AC. 2009. Expression of the *sarA* family of genes in different strains of *Staphylococcus aureus*. *Microbiology* 155:2342–2352. <https://doi.org/10.1099/mic.0.027417-0>.
  78. Jefferson KK, Cramton SE, Gotz F, Pier GB. 2003. Identification of a 5-nucleotide sequence that controls expression of the *ica* locus in *Staphylococcus aureus* and characterization of the DNA-binding properties of IcaR. *Mol Microbiol* 48:889–899.
  79. Waters EM, McCarthy H, Hogan S, Zapotoczna M, O'Neill E, O'Gara JP. 2014. Rapid quantitative and qualitative analysis of biofilm production by *Staphylococcus epidermidis* under static growth conditions. *Methods Mol Biol* 1106:157–166.
  80. Olson ME, Slater SR, Rupp ME, Fey PD. 2010. Rifampicin enhances activity of daptomycin and vancomycin against both a polysaccharide intercellular adhesin (PIA)-dependent and -independent *Staphylococcus epidermidis* biofilm. *J Antimicrob Chemother* 65:2164–2171. <https://doi.org/10.1093/jac/dkq314>.
  81. Serrano M, Zilhao R, Ricca E, Ozin AJ, Moran CP, Jr, Henriques AO. 1999. A *Bacillus subtilis* secreted protein with a role in endospore coat assembly and function. *J Bacteriol* 181:3632–3643.
  82. Hamon MA, Stanley NR, Britton RA, Grossman AD, Lazazzera BA. 2004. Identification of AbrB-regulated genes involved in biofilm formation by *Bacillus subtilis*. *Mol Microbiol* 52:847–860. <https://doi.org/10.1111/j.1365-2958.2004.04023.x>.
  83. Ryjenkov DA, Tarutina M, Moskvina OV, Gomelsky M. 2005. Cyclic diguanylate is a ubiquitous signaling molecule in bacteria: insights into biochemistry of the GGDEF protein domain. *J Bacteriol* 187:1792–1798. <https://doi.org/10.1128/JB.187.5.1792-1798.2005>.
  84. Sasakura Y, Hirata S, Sugiyama S, Suzuki S, Taguchi S, Watanabe M, Matsui T, Sagami I, Shimizu T. 2002. Characterization of a direct oxygen sensor heme protein from *Escherichia coli*: effects of the heme redox states and mutations at the heme-binding site on catalysis and structure. *J Biol Chem* 277:23821–23827. <https://doi.org/10.1074/jbc.M202738200>.
  85. Holland LM, O'Donnell ST, Ryjenkov DA, Gomelsky L, Slater SR, Fey PD, Gomelsky M, O'Gara JP. 2008. A staphylococcal GGDEF domain protein regulates biofilm formation independently of cyclic dimeric GMP. *J Bacteriol* 190:5178–5189. <https://doi.org/10.1128/JB.00375-08>.
  86. Du B, Ji W, An H, Shi Y, Huang Q, Cheng Y, Fu Q, Wang H, Yan Y, Sun J. 2014. Functional analysis of c-di-AMP phosphodiesterase, GdpP, in *Streptococcus suis* serotype 2. *Microbiol Res* 169:749–758. <https://doi.org/10.1016/j.micres.2014.01.002>.
  87. Corrigan RM, Abbott JC, Burhenne H, Kaefer V, Grundling A. 2011. c-di-AMP is a new second messenger in *Staphylococcus aureus* with a role in controlling cell size and envelope stress. *PLoS Pathog* 7:e1002217. <https://doi.org/10.1371/journal.ppat.1002217>.
  88. Peng X, Zhang Y, Bai G, Zhou X, Wu H. 2016. Cyclic di-AMP mediates biofilm formation. *Mol Microbiol* 99:945–959. <https://doi.org/10.1111/mmi.13277>.
  89. Townsley L, Yannarell SM, Huynh TN, Woodward JJ, Shank EA. 2018. Cyclic di-AMP acts as an extracellular signal that impacts *Bacillus subtilis* biofilm formation and plant attachment. *mBio* 9:e00341-18. <https://doi.org/10.1128/mBio.00341-18>.
  90. Galdbart JO, Allignet J, Tung HS, Ryden C, El Solh N. 2000. Screening for *Staphylococcus epidermidis* markers discriminating between skin-flora strains and those responsible for infections of joint prostheses. *J Infect Dis* 182:351–355. <https://doi.org/10.1086/315660>.
  91. Wojtyczka RD, Orlewska K, Kępa M, Idzik D, Dziedzic A, Mularz T, Krawczyk M, Mikłasińska M, Wąsik TJ. 2014. Biofilm formation and antimicrobial susceptibility of *Staphylococcus epidermidis* strains from a hospital environment. *Int J Environ Res Public Health* 11:4619–4633. <https://doi.org/10.3390/ijerph110504619>.
  92. Oliveira A, Cunha M. 2010. Comparison of methods for the detection of biofilm production in coagulase-negative staphylococci. *BMC Res Notes* 3:260. <https://doi.org/10.1186/1756-0500-3-260>.
  93. Arciola CR, Baldassarri L, Montanaro L. 2001. Presence of *icaA* and *icaD* genes and slime production in a collection of staphylococcal strains from catheter-associated infections. *J Clin Microbiol* 39:2151–2156. <https://doi.org/10.1128/JCM.39.6.2151-2156.2001>.
  94. Mack D, Siemssen N, Laufs R. 1992. Parallel induction by glucose of adherence and a polysaccharide antigen specific for plastic-adherent *Staphylococcus epidermidis*: evidence for functional relation to intercellular adhesion. *Infect Immun* 60:2048–2057.
  95. Augustin J, Gotz F. 1990. Transformation of *Staphylococcus epidermidis* and other staphylococcal species with plasmid DNA by electroporation. *FEMS Microbiol Lett* 54:203–207.



96. Kreiswirth BN, Lofdahl S, Betley MJ, O'Reilly M, Schlievert PM, Bergdoll MS, Novick RP. 1983. The toxic shock syndrome exotoxin structural gene is not detectably transmitted by a prophage. *Nature* 305:709–712. <https://doi.org/10.1038/305709a0>.
97. Winstel V, Kuhner P, Krismer B, Peschel A, Rohde H. 2015. Transfer of plasmid DNA to clinical coagulase-negative staphylococcal pathogens by using a unique bacteriophage. *Appl Environ Microbiol* 81:2481–2488. <https://doi.org/10.1128/AEM.04190-14>.
98. Olson ME, Horswill AR. 2014. Bacteriophage Transduction in *Staphylococcus epidermidis*. *Methods Mol Biol* 1106:167–172. [https://doi.org/10.1007/978-1-62703-736-5\\_15](https://doi.org/10.1007/978-1-62703-736-5_15).
99. Vuong C, Otto M. 2008. The biofilm exopolysaccharide polysaccharide intercellular adhesin—a molecular and biochemical approach. *Methods Mol Biol* 431:97–106.
100. Christensen GD, Simpson WA, Bisno AL, Beachey EH. 1982. Adherence of slime-producing strains of *Staphylococcus epidermidis* to smooth surfaces. *Infect Immun* 37:318–326.
101. Studier FW, Moffatt BA. 1986. Use of bacteriophage T7 RNA polymerase to direct selective high-level expression of cloned genes. *J Mol Biol* 189:113–130.
102. Snesrud E, Ong AC, Corey B, Kwak YI, Clifford R, Gleeson T, Wood S, Whitman TJ, Lesho EP, Hinkle M, Mc Gann P. 2017. Analysis of serial isolates of *mcr-1*-positive *Escherichia coli* reveals a highly active IS*ApI1* transposon. *Antimicrob Agents Chemother* 61:e00056-17. <https://doi.org/10.1128/AAC.00056-17>.